HAL
open science

Surface photovoltage characterisation of metal halide perovskite on crystalline silicon using Kelvin probe force microscopy and metal-insulator-semiconductor configuration

Aleksandra Bojar, Davide Regaldo, J Alvarez, David Alamarguy, Vesselin Donchev, Stefan Georgiev, Philip Schulz, Jean Paul Kleider

To cite this version:

Aleksandra Bojar, Davide Regaldo, J Alvarez, David Alamarguy, Vesselin Donchev, et al.. Surface photovoltage characterisation of metal halide perovskite on crystalline silicon using Kelvin probe force microscopy and metal-insulator-semiconductor configuration. EPJ Photovoltaics, 2022, 13, pp.18. 10.1051/epjpv/2022016 . hal-03749484

HAL Id: hal-03749484

https://hal.science/hal-03749484v1

Submitted on 10 Aug 2022

HAL is a multi-disciplinary open access archive for the deposit and dissemination of scientific research documents, whether they are published or not. The documents may come from teaching and research institutions in France or abroad, or from public or private research centers.

L'archive ouverte pluridisciplinaire **HAL**, est destinée au dépôt et à la diffusion de documents scientifiques de niveau recherche, publiés ou non, émanant des établissements d'enseignement et de recherche français ou étrangers, des laboratoires publics ou privés.

EPJ Photovoltaics **13**, 18 (2022)
© A. Bojar et al., Published by EDP Sciences, 2022
https://doi.org/10.1051/epjpv/2022016

Available online at:
www.epj-pv.org

Special Issue on 'Recent Advances in Spectroscopy and Microscopy of Thin-films Materials, Interfaces, and Solar Cells 2021', edited by A. Vossier, M. Gueunier-Farret, J.-P. Kleider and D. Mencaraglia

Regular Article

Open Access

Surface photovoltage characterisation of metal halide perovskite on crystalline silicon using Kelvin probe force microscopy and metal-insulator-semiconductor configuration

Aleksandra Bojar[1,2,3,*], Davide Regaldo[1,2,3], José Alvarez[2,3], David Alamarguy[2,3], Vesselin Donchev[4], Stefan Georgiev[4], Philip Schulz[1,5], and Jean-Paul Kleider[1,2,3]

[1] IPVF, Institut Photovoltaïque d'Ile-de-France, 18, Boulevard Thomas Gobert, 91120 Palaiseau, France
[2] Université Paris-Saclay, CentraleSupélec, CNRS, Laboratoire de Génie Electrique et Electronique de Paris, 91192 Gif-sur-Yvette, France
[3] Sorbonne Université, CNRS, Laboratoire de Génie Electrique et Electronique de Paris, 75252 Paris, France
[4] Faculty of Physics, Sofia University, blvd. James Bourchier, 5, 1164 Sofia, Bulgaria
[5] CNRS, École Polytechnique, IPVF, UMR 9006, 18, Boulevard Thomas Gobert, 91120 Palaiseau, France

Received: 28 March 2022 / Received in final form: 17 May 2022 / Accepted: 13 June 2022

Abstract. In this study we analysed halide perovskite films deposited directly on crystalline silicon by means of two set-ups using different operating modes of the surface photovoltage (*SPV*) methods, i.e., the Kelvin probe force microscopy (KPFM) and the metal-insulator-semiconductor (MIS) technique. The KPFM allowed to visualize surface potential distribution on a microscale while MIS technique allowed to study *SPV* spectral dependence. We studied wavelength dependent *SPV* of these samples, which allowed us to effectively vary the probe depth in the sample and discern the contribution from each interface to the overall effect measured under white light illumination. Depending on where the photocarriers are generated, different *SPV* signals are observed: at the perovskite/Si interface, the signal depends on Si doping type, while at the surface the *SPV* is always negative indicating downward surface band bending. This is confirmed by analysing *SPV* phase measured in the AC MIS mode. In addition, distinction between slow and fast processes contributing to measured *SPV* was possible. It has been observed, that with decreasing the illumination wavelength, the processes causing *SPV* become slower, which can indicate that high energy photons not only generate electronic photocarriers but can also induce chemical changes with creation of defects or ionic species that also modify the measured *SPV*.

Keywords: Surface photovoltage / Kelvin probe force microscopy / metal halide perovskites / metal-insulator-semiconductor

1 Introduction

Perovskite-silicon tandem solar cells are a promising way for overcoming the single-cell efficiency limit. To date, only a few studies were dedicated to a direct investigation of immediate perovskite-silicon interface [1–6]. While in most tandem solar cell designs these two materials are not in direct contact, knowledge of the carrier transport and band alignment at their interface would allow for a better understanding of their compatibility and attainable performance levels, guiding the development of perovskite-silicon tandem solar cells in monolithic device architectures with adapted tunnel-recombination junctions between the two sub-cells.

The surface photovoltage (*SPV*) technique consists of measuring the changes of the surface potential, which are induced by optical generation of free charge carriers, followed by their space redistribution in the sample. It gives information regarding band bending in the sample both at the surface and interfaces, and thus opens the discussion on band alignment between materials.

Our approach was based on producing samples of perovskite directly deposited on crystalline silicon substrate via spin coating method. We have chosen triple cation mixed halide perovskite due to its superior properties over $MAPbI_3$ [7], and silicon substrate of p-type (p-Si)

* e-mail: aleksandra.bojar@cnrs.fr

This is an Open Access article distributed under the terms of the Creative Commons Attribution License (https://creativecommons.org/licenses/by/4.0), which permits unrestricted use, distribution, and reproduction in any medium, provided the original work is properly cited.

and n-type (n-Si) doping. Then, we used surface photovoltage effect to gain some insights about the charge carrier transport in this material system. For this, we used two different configurations to measure the *SPV*, namely metal-insulator-semiconductor configuration and Kelvin probe force microscopy. Regarding the former, we measured *SPV* in the broad illumination wavelength range, from 900 to 500 nm. Regarding the latter, we used three different illumination wavelengths to be able to induce the *SPV* effect in different regions in the sample. Based on the absorption spectra of our perovskite and its band gap measured by PL, the infrared illumination is passing through perovskite layer to be finally absorbed in the silicon below. *SPV* measured with the use of this illumination will originate mostly from the buried interface band bending. On the other hand, blue illumination is fully absorbed at the perovskite surface due to strong absorption coefficient at this photon energies and will provide us with the information about the band bending present at the perovskite surface.

In KPFM, conducting AFM tip acquires the topography image and surface potential distribution simultaneously, which can be done both in the dark and under laser illumination. The measured parameter in this method is a contact potential difference, *CPD*, which reflects the potential at the sample's surface. By subtracting the *CPD* measured in the dark from the one measured under illumination, we obtain the *SPV* magnitude and sign (that is the sign of the charge carriers, either electronic or ionic, that were moving toward the surface where the measurement is done). The *SPV* is the measure of the separation of photogenerated charge carriers in space [8–12]. The value of *SPV* is proportional to the number of separated carriers, while its sign indicates the type of carriers that moved towards the surface, where the *SPV* is measured. Equivalently, that means that it provides us with the magnitude and the direction of the band bending. Downward band bending is flattening under illumination due to electrons moving towards the surface. The measured *SPV* will be negative in this case. Similar principle applies to the buried interface band bending. The opposite is true in case of upward band bending.

An alternative way of measuring the *SPV* can be done in metal-insulator-semiconductor configuration [13–15]. Here, plate capacitor is formed, which is then charged and brought to open circuit conditions. The structure is illuminated with a chopped light with sufficiently high frequency to avoid gradual discharge of the capacitor, and the excitation reaching the sample can be expressed by $I_0\cos(\omega t)$, where I_0 is the incoming light intensity and ω is the frequency of the chopper. The change of the surface potential due to photovoltaic effect results in equivalent voltage change between the plates of the capacitor. The *SPV* at the insulator semiconductor interface is measured by lock in amplifier and can be expressed by $SPV\cos(\omega t\text{-}\varphi)$, where *SPV* is the amplitude of the measured signal and φ is its phase. Based on [13,14] we can interpret the amplitude *SPV* as the equivalent of the magnitude of the surface photovoltage measured by KPFM, while the phase as the equivalent to the sign of the *SPV*. The phase located between 0° and 90° and 0° and −90° corresponds to the positive sign of the *SPV*, while the phase located between 90° and 180° and −90° and −180° corresponds to the negative sign of the *SPV*.

2 Results and discussion

2.1 Sample production

Triple cation mixed halide perovskite thin films were deposited via spin-coating method directly on c-Si substrates of p-type and n-type doping type. Material and procedure details can be found in the supporting information (SI). The preparation of the c-Si surface turned out to be crucial for the successful perovskite deposition, and 30 min of the ultraviolet-ozone treatment provided the sufficient hydrophilicity of the surface to obtain full and homogenous coverage. The perovskite layers quality has been then assessed using X-ray diffraction (XRD), scanning electron microscopy (SEM), ultraviolet photoemission spectroscopy (UPS) and photoluminescence (PL). The results are shown in the SI. In brief, the SEM images, as well as the photo on the Figure S1 reveal that the perovskite layer fully and quite homogenously covered silicon surface, providing a high-quality surface for further examination. The film thickness was between 400 and 500 nm, as expected form production parameters. Presence of another phase can be seen on backscattered electron image, where brighter grains indicate probably PbI_2 phase. This is expected, as the perovskite solution was prepared with PbI_2 excess to increase material performance, as reported in the literature [16], and used in the baseline perovskite solar cell production in our institute. The XRD results (Fig. S2) revealed highly crystalline nature of the perovskite film exhibiting the perovskite phase as the dominant one. The small amounts of the foreign phase have been observed and it has been identified as PbI_2 phase. The presence of strong peak around 70° has been observed and it corresponds to the substrate main plane family <100>. The band gap of perovskite film was determined using photoluminescence measurements, and it is 1.63 eV. Important to note is that there were no differences in these measurements between perovskite deposited on p-type or n-type silicon: structural and morphological properties of the film as well as the band gap were not depended on the silicon-substrate doping type.

Figure 1 shows the normalised photoluminescence (PL) represented by the green peak, and normalised absorbance (black dashed line) obtained from spectroscopic ellipsometry measurements. The graph also contains the wavelengths of the lasers used in KPFM surface photovoltage experiments, namely 488 nm, 785 nm and 980 nm. They are represented by the vertical pink dotted lines. This allowed us to estimate the absorption process of each of the four wavelengths in the PVK/c-Si system. The laser of 488 nm will be quickly absorbed by the perovskite surface due to very strong absorbance at these wavelengths. The 785 nm laser will be absorbed by perovskite bulk, but some part of it will be transferred to the c-Si substrate. Finally, the 980 nm laser will not be absorbed by the perovskite, and thus it will be fully transmitted to and absorbed by the c-Si. The wavelength dependence of the perovskite photovoltage and potential response has been reported in the literature [17–21]. The idea of probing different regions of the sample using various illumination wavelengths is not new [22] but implemented for the first time to probe direct interface

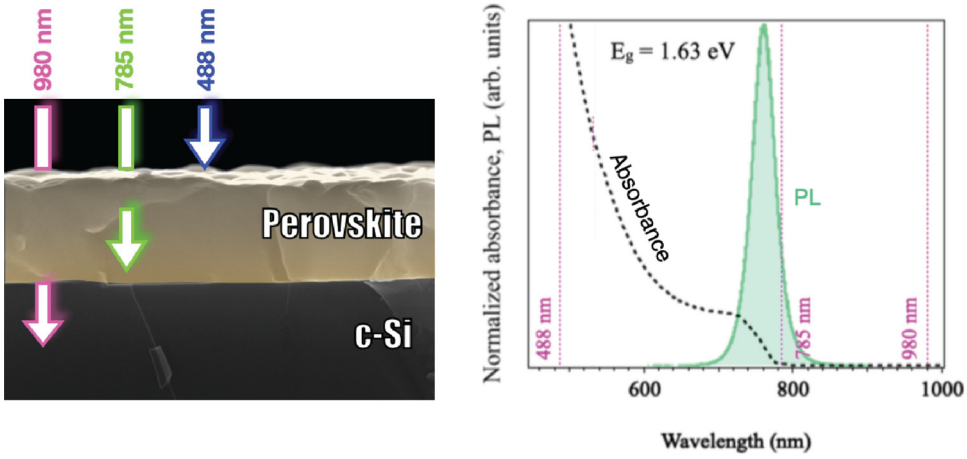

Fig. 1. The idea of the experiments performed in this work: the use of the laser of different wavelengths allows to induce *SPV* effect in different regions of the sample. Based on PL/absorbance results showed on the graph, the 980 nm illumination is not absorbed by PVK layer but only by c-Si below and on the other hand the 488 nm laser is absorbed mostly at the perovskite surface.

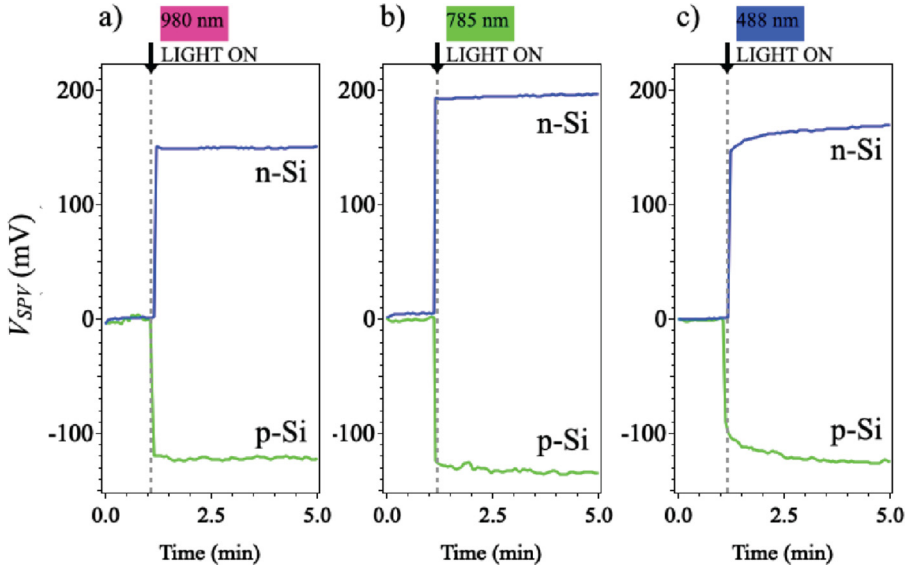

Fig. 2. The *SPV* results measured on bare c-Si substrates (n-type blue and p-type green) using KPFM method. The direction of *SPV* does not depend on the illumination wavelength and results in positive *SPV* for n-Si and negative SPV for p-Si.

between perovskite and crystalline silicon. Here, both materials are absorbers of different parts of the illumination spectrum, thus depending on where the light is absorbed the carriers can be generated either in silicon, in perovskite bulk or at the perovskite surface. Furthermore, highly energetic photons can induce other effects than electronic ones, which will be also discussed in this work.

2.2 KPFM results

Firstly, we measured the wavelength dependent *SPV* of the bare c-Si substrate. The results of the measurements are shown in Figure 2.

On Figure 2a we can see the change in the surface potential induced by the infrared illumination (980 nm) for n-Si (blue line) and p-Si (green line). The n-Si shows positive value of $SPV \approx 0.15$ V, while p-Si shows negative value of $SPV \approx -0.12$ V. In c-Si wafer the only region where the electrostatic field can exist is the surface space charge region. Majority charge carriers get trapped at the surface states leading to the depletion at the surface (reduced density of the majority carriers in comparison to its equilibrium value). For n-Si, electrons are captured by the surface states and the upward band bending is formed. Under illumination, electron-hole pairs are created and separated by the built-in field due to this band bending. The electrons move towards the bulk, and holes towards the surface, where they neutralize the surface state reducing the band bending. This is usually observed as an increase of the surface potential value (in the situation

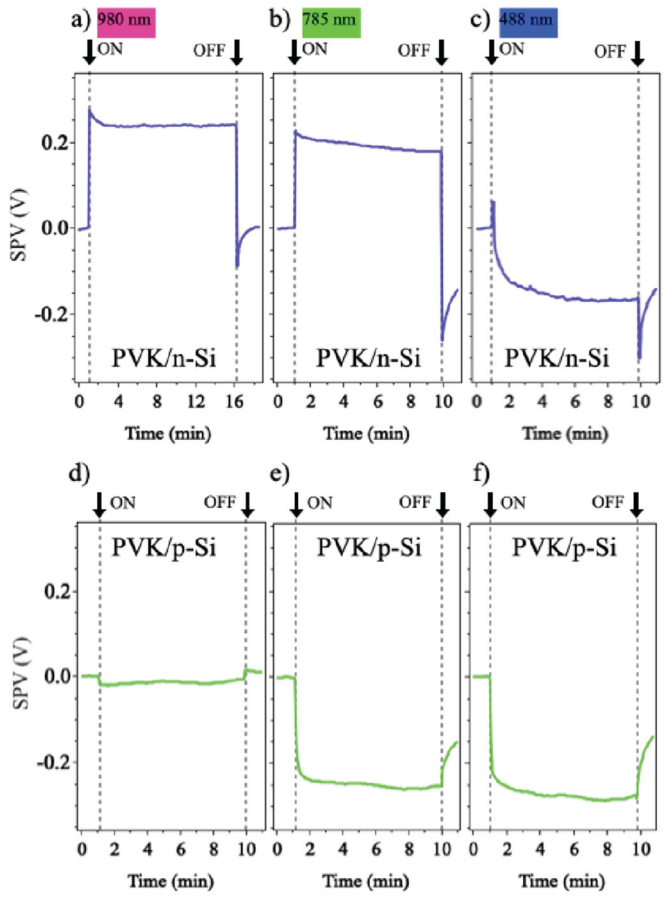

Fig. 3. The *SPV* measurements of the PVK/c-Si samples using different illumination wavelengths. Results for PVK/n-Si are shown on a-c and for PVK/p-Si on d-f. The dashed grey lines indicates when the light was turned on and off.

where the sample is grounded), and thus − positive *SPV*. The opposite is true in case of the downward band bending in p-type semiconductors. In other words, the sign of *SPV* is determined by the type of charge carriers separated towards the surface [9]. We can clearly see this effect in case of the bare c-Si substrates. To illustrate described processes drift-diffusion simulations have been done and are shown in the SI. Similar processes take place also under 785 nm and 488 nm illuminations, and their magnitudes.

Next, we performed the same measurements of the samples with perovskite on top, and the results are shown in Figure 3. In this case, the measurement of *SPV* is much more complex due to the numerous possible reasons that can result in rise of *SPV*, including processes occurring both at the surface and at the interface. In a sample containing a thin layer deposited on the surface, the energy bands are serially connected [10,12]. Thus, *SPV* measured at the physical surface of the sample, reveals information on the nature of bulk, surface and interfacial properties and processes of the system, which include charge carrier recombination, accumulation, trapping/de-trapping, carrier decay dynamics and ionic processes [12]. The sign of *SPV* of such structures will be then determined by the dominant component (surface or interface). The surface potential changes under illumination for PVK/n-Si are shown on (a-c) and for PVK/p-Si on (d-f).

As explained at the beginning, in our strategy we used different illumination wavelength to probe different regions of the sample. Here, we can see the *SPV* induced by near-infrared illumination (980 nm) that is absorbed only in silicon. It provides us with the interface characteristics, and we can see significant differences in the *SPV* depending on the substrate doping type. When perovskite is deposited on p-type silicon, *SPV* is negligible, slightly negative, indicating little to no charge carrier separation at the interface. On the other hand, the interface between n-Si and PVK allows the positive carriers (holes) to move towards the surface, where the *SPV* is measured, which results in a positive sign. Some charges can be trapped at the interface defects, which is visible as a small decrease of the *SPV* a few seconds after illumination was turned on. When the filling of defect traps has reached a steady-state, the *SPV* remains constant for the remaining time of illuminated measurements. The trapped carriers manifest their presence by the negative peak just after turning off the illumination. Their trap release can be observed as a slow return to the initial value. No ionic movement is involved here. The drift diffusion simulations of the *SPV* and the band diagrams of the structures are included in the SI to better illustrate the discussion.

According to the absorption spectra of the perovskite (Fig. 1b), the 785 nm illumination is absorbed by perovskite, but not very strong, so it can penetrate its bulk and even be absorbed partially by silicon. In this case, measured *SPV* will be the sum of the interface and surface contributions, and it is negative in case of perovskite on p-type silicon and positive in case of perovskite on n-type silicon. More specifically, in the case of perovskite on p-Si, the interface contribution is negligible (Fig. 3d), thus the *SPV* under 785 nm is mostly originating from the perovskite contribution, indicating a movement of negatively charged carriers, either ions or electrons, towards the surface. For PVK/n-Si, under 785 nm the *SPV* magnitude is smaller and also it starts to include the negative component of the perovskite surface. Trapping of carriers in this case at the interface is also probably present, as in case of 980 nm illumination, but a small ionic component causes the *SPV* constantly decrease with time, as negatively charged ions are slowly accumulating close to the perovskite surface. Their slower movement when the light was turned off is also seen as a much slower return to the initial value than the 980 nm.

The blue illumination provides us with very important information regarding perovskite surface. We can see, that in both samples, the *SPV* is negative, meaning that the surface band bending promotes the movement of negative charge carriers towards the surface. In other words, the results indicate significant downward band bending at the perovskite surface regardless of the substrate doping type. This band bending can be caused by presence of donor states from reduced lead centres [21,23–25]. This can also explain the fact, that the perovskite looks very n-type in both cases, as we could see in the UPS results (see Fig. S3).

We can observe, that after illumination with 980 nm infrared light, the surface potential relaxes back to its original value within 1–2 min. (Figs. 3a and 3d), meaning that the

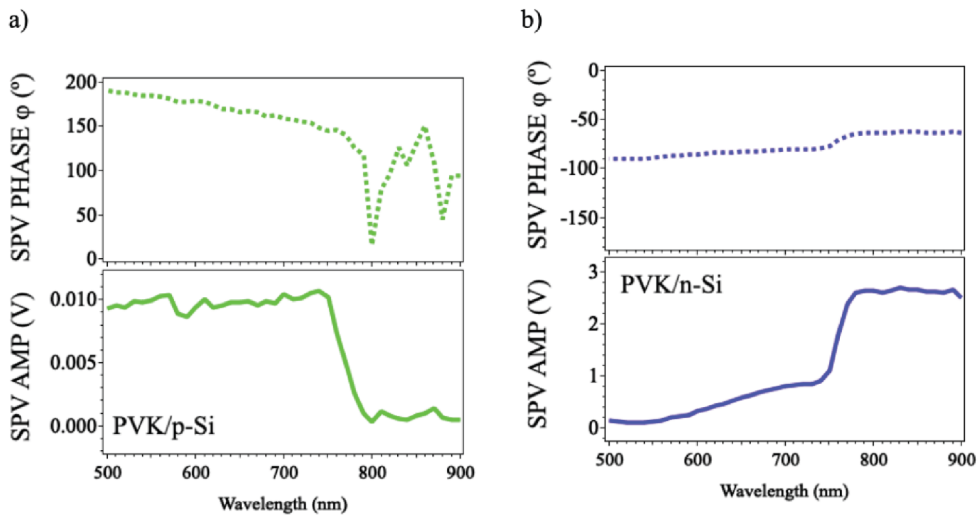

Fig. 4. The *SPV* results of PVK/p-SI (a) and PVK/n-Si (b) measured by MIS technique. The top graph shows *SPV* phase, and the bottom graph shows *SPV* amplitude.

residual *SPV* value two minutes after the light was turned off is then 0 V. In case of 785 nm illumination, two minutes are not enough to return to the initial equilibrium value measured in the dark (within the measurement error). We observe residual *SPV* of ≈0.09 V for the PVK/p-Si sample and ≈0.04 V for the PVK/n-Si sample. What needs to be underlined here, is that no matter what the initial sign of *SPV* was, after turning off the light there is always a remaining negative value, which then slowly goes toward zero. The slow relaxation after 785 nm illumination for the PVK/p-Si sample can be caused by the electrons generated in perovskite that might have been left with no holes to recombine, indicating good extraction of holes at the PVK/p-Si interface. Moreover, the fast negative change in *SPV* followed by slower change toward zero (equilibrium value) for the PVK/n-Si sample after switching off 785 nm illumination probably includes ionic redistribution and accumulation in perovskite. In case of blue illumination, the *SPV* residue after 2 min is quite high in both samples (0.13 V for PVK/p-Si and 0.15 V for PVK/n-Si), revealing significant persistent photovoltage related to very slow relaxation and or (semi-)permanent modification of the surface potential.

2.3 MIS results

Next, we investigated wavelength dependence of the surface photovoltage of the PVK/c-Si samples using surface photovoltage spectroscopy (SPS), which is a technique that measures the surface potential changes in the broad range of wavelengths. This technique has been developed in the metal-insulator-semiconductor (MIS) configuration in AC. The goal was to complement the KPFM-based measurements of *SPV* with the advantages that offers the MIS technique, and furthermore, to analyse PVK/c-Si materials using this operation mode, which to our knowledge, has not been done before.

As explained in the previously, this technique can measure simultaneously the amplitude and the phase of *SPV*. The amplitude gives information about the number of separated charge carriers, while the phase can be related to the sign of the signal one would have under DC conditions. It also contains information about how fast the process is [13–15].

The results of the AC SPS measurements on the PVK/p-Si sample using the MIS technique are shown in Figure 4. For the sample PVK/p-Si we observe negligible amplitude in the sub-band gap region, that increases sharply when the wavelength reaches the energy gap region. Regarding the phase changes for this sample, in the infrared region it is equivalent of the negative sign of *SPV* in KPFM measurements.

Regarding the *SPV* spectra of the PVK/n-Si sample, in the infrared region the *SPV* amplitude is the highest. With the decrease of the illumination wavelength, the amplitude decreases, reaching a value below 1 mV under 500 nm illumination. Regarding the phase, it remains all the time between 0° and −90°, which corresponds to positive sign of the *SPV*. The change of the phase when decreasing the wavelength (increasing the photon energy) means, that the processes causing *SPV* have higher phase retardation, meaning, they occur in slower time scales.

For both samples we observe a change of the *SPV* phase with the illumination from low energy to high energy photons. This is accompanied by the change of the absorption region, as discussed before: for the infrared illumination only silicon substrate absorbs, while for shorter wavelengths perovskite material adds its contribution to the *SPV*. For highly energetic photons we must also consider ionic effects and /or degradation processes, as it was discussed in case of KPFM results. However, what needs to be kept in mind is the difference of the techniques. First, the KPFM measures the surface potential in the dark and then under illumination; the *SPV* is obtained by subtracting the dark potential from the one measured under illumination. On the other hand, MIS measures directly (and only) the changes of the surface potential under illumination/dark. In this case, there is a very short period of illumination followed by short time in the dark.

Speaking straightforward, the KPFM and MIS techniques can capture the processes at the different time scales – in KPFM we can observe the effects of slow processes on the SPV, but we are not able to resolve well fast processes. On the other hand, AC MIS technique can provide us with information related to the fast processes that causes SPV, but it is not able to measure slow ones, that requires seconds or even minutes to develop under constant illumination. This makes the results from the two techniques not immediately comparable, but it provides a perfect way to complement the KPFM results with the advantages of the AC MIS technique, allowing to gain more complete picture of the processes occurring in the sample under illumination with different wavelengths and at different time scales.

The MIS technique is not able to measure the effects of such slow processes, however the clockwise rotation of the vector for PVK/n-Si indicates that under higher photon energy illumination, the processes are slower. Thus, we can see that as soon as perovskite starts to absorb light and contribute to SPV, the slow processes need to be considered. This supports further the ionic motion or chemical creation of charged species in perovskite under illumination, which redistribution leads to the changes in measure SPV over the time.

3 Conclusions

In summary, based on this analysis the PVK induces negative SPV, independently on the substrate that it is deposited on. It supports the hypothesis of the existence of the downward band bending at the perovskite surface, that we used for the explanation of KPFM data, and it was also observed in UPS measurements where the valence band to Fermi level distance values were indicating n-type character of the PVK surface. Downward band bending at the PVK surface was also often reported in the literature [26–28]. The long-term effects like ion migration or PVK surface decomposition cannot be observed in the AC MIS technique due to operation mode and high frequencies used. Thus, by taking advantage of the complementary aspect of the AC MIS technique, we were able to complement the information obtained from the KPFM data and support the corresponding discussion.

Supplementary material

Supporting information provided by the authors. The Supplementary Material is available at https://www.epjpv.org/10.1051/epjpv/2022016/olm.

This work was carried out in the frame of the PERMAVOLT project of the French-Bulgarian PHC RILA 2022 programme (КП-06-Рила/10 /16.12.2021 and N°48059QL). It was also supported by the European Regional Development Fund within the Operational Program "Science and Education for Smart Growth 2014–2020" under the Project CoE "National center of mechatronics and clean technologies "BG05M2OP001-1.001-0008, as well as by the French government in the frame of the program of investments for the future (Programme d'investissement d'Avenir ANR-IEED-002-01). P.S. thanks the French Agence Nationale de la Recherche for funding under the contract number ANR-17-MPGA-0012.

Author contribution statement

Supervision: PS, JPK; writing (original draft): AB; writing (revisions and editing): AB, JPK, VD, PS; visualisation: AB; result analysis: AB, DR, VD, JPK, PS; discussion: AB, DR, JA, DA, VD, SG, PS, JPK; sample production: AB, experiments: AB (KPFM, PL, SEM, XRD, UPS); VD & SG (MIS), DA (UPS, XPS), simulations (DR).

References

1. N.F. Rostan et al., Surf. Interface Anal. **52**, 422 (2020)
2. N.F. Rostan et al., AIP Conf. Proc. **1838**, 020020 (2017)
3. K.S. Sekerbayev et al., Jetp Lett. **110**, 592 (2019)
4. K.S. Sekerbayev et al., Physica B **582**, 412025 (2020)
5. R. Gonzalez-Rodriguez et al., Nanoscale **12**, 4498 (2020)
6. S. Mariotti et al., IEEE J. Photovolt. **10**, 945 (2020)
7. M. Saliba et al., Energy Environ. Sci. **9**, 1989 (2016)
8. L. Barnea-Nehoshtan et al., J. Phys. Chem. Lett. **5**, 2408 (2014)
9. R. Chen et al., Chem. Soc. Rev. **47**, 8238 (2018)
10. L. Kronik, Y. Shapira, Surf. Sci. Rep. **37**, 1 (1999)
11. C. Lu et al., Adv. Mater. Interfaces **6**, 1801253 (2019)
12. M. Daboczi et al., ACS Appl. Mater. Interfaces **11**, 46808 (2019)
13. V. Donchev et al., Trends Appl. Spectrosc. **8**, 27 (2010)
14. V. Donchev, Mater. Res. Express **6**, 103001 (2019)
15. Cavalcoli et al., Phys. Status Solidi C **7**, 1293 (2010)
16. T. Du et al., Sustain. Energy Fuels **1**, 119 (2017)
17. E.M. Tennyson et al., Chem. Mater. **31**, 8969 (2019)
18. M. Pazoki et al., J. Phys. Chem. C **121**, 26180 (2017)
19. W.A. Quitsch et al., J. Phys. Chem. Lett. **9**, 2062 (2018)
20. W. Ma et al., J. Mater. Sci. **52**, 9696 (2017)
21. F.S. Zu et al., Adv. Optical Mater. **2017**, 1700139 (2017)
22. E.M. Tennyson et al., ACS Energy Lett. **1**, 899 (2016)
23. S.P. Dunfield et al., Cell Reports Phys. Sci. **2**, 2666 (2021)
24. U.B. Cappel et al., ACS Appl. Mater. Interfaces **9**, 34970 (2017)
25. Q. Sun et al., Adv. Energy Mater. **7**, 1700977 (2017)
26. P. Caprioglio et al., Sustain. Energy Fuels **3**, 550 (2019)
27. T. Gallet et al., Nanoscale **11**, 16828 (2019)
28. F.S. Zu et al., ACS Appl. Mater. Interfaces **11**, 21578 (2019)

Cite this article as: Aleksandra Bojar, Davide Regaldo, José Alvarez, David Alamarguy, Vesselin Donchev, Stefan Georgiev, Philip Schulz, Jean-Paul Kleider, Surface photovoltage characterisation of metal halide perovskite on crystalline silicon using Kelvin probe force microscopy and metal-insulator-semiconductor configuration, EPJ Photovoltaics **13**, 18 (2022)